Lubrication Analysis and Boundary Integral Simulations of a Viscous Micropump

R.F. Day and H.A. Stone

Division of Engineering & Applied Sciences, Harvard University
Pierce Hall, 29 Oxford Street, Cambridge, MA 02138
tel: (617)496-1460, fax: (617)495-9837
email: rfday@deas.harvard.edu, has@deas.harvard.edu

ABSTRACT

Several recent papers discuss a novel viscous micropump consisting of Poiseuille flow of fluid between two plates and a cylinder placed along the gap perpendicular to the flow direction. If the cylinder is not centered, rotating it will generate a net flow and a pressure drop along the channel, due to the net tangential viscous stresses along its surface. This device was proposed and demonstrated experimentally by Sen et al. [1], and has been simulated with finite-elements by Sharatchandra et al. [2] and DeCourtye et al. [3]. The research reported here complements their work by examining the lubrication limit where the gaps between the cylinder and the walls are small compared to the cylinder radius. Lubrication analysis shows there are optimum gap ratios for the maximum rotation rate and the maximum bulk flow. Also, since the Reynolds number can be much less than one, the Stokes equations are solved numerically, using a boundary integral method.

Keywords: MEMS, Lubrication, Boundary Integral, Stokes

Introduction

The recent study of micro-electro-mechanical systems (MEMS) has generated great interest in the design and demonstration of micropumps and micromotors. Sen et al. [1] proposed and demonstrated experimentally a viscous micropump that uses a cylinder to generate flow between two plates. The device has been studied numerically by Sharatchandra et al. [2] using 2D finite-element methods, and recently by Decourtye et al. [3] using 3D finite-element software.

The research reported here complements the above work by using modeling and simulation methods specific to thin gaps and low-Reynolds-number flows. This paper addresses the lubrication limit of the viscous micropump, and investigates the Stokes flow problem since the Reynolds number of the flow based on the cylinder radius can be much less than one. The resulting Stokes equations are solved using a boundary integral method, thus eliminating the problem of insufficient mesh generation in the gaps, as is often encountered in finite-element methods.

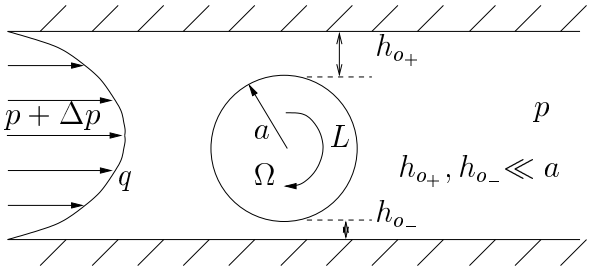

Figure 1: Sketch of viscous micropump/micromotor where the flow upstream and downstream is parabolic.

Consider Poiseuille flow of fluid in the space between two plates. A cylinder is introduced perpendicular to the flow and parallel to the walls. If the cylinder is not centered in the gap, it will tend to rotate due to the net tangential viscous stresses along the surface of the cylinder, as shown in Figure 1. Conversely, if the eccentrically-placed cylinder is rotated by a torque, it will generate a flow in the channel, and an accompanying pressure drop across the cylinder. Four flow parameters characterize the flow: flow rate per unit width q, rotation rate Ω, pressure drop Δp, and torque L. A pump and motor are the same device, but with different input and output parameters. For example, given Δp and torque L, one can determine a rotation rate and a flow through the device. This would effectively be a motor where the cylinder is connected to a certain load. It is of interest to calculate what the relationships are between these quantities, and it will be shown that lubrication analysis achieves a satisfactory solution, where the regime of applicability of lubrication theory is shown by full boundary integral solutions of the Stokes equations.

Since Stokes flows are linear, we can immediately say that there must be a linear relationship between the four parameters q, Ω, Δp, and L described by a matrix of coefficients,

$$\mu \begin{bmatrix} A_{q\Delta p} & A_{\Omega\Delta p} \\ A_{qL} & A_{\Omega L} \end{bmatrix} \begin{pmatrix} q \\ \Omega \end{pmatrix} = \begin{pmatrix} \Delta p \\ L \end{pmatrix} \tag{1}$$

where the A's are functions of geometry. The matrix elements can be found directly using lubrication analysis, and can be found numerically using the boundary integral method.

Lubrication analysis

Consider the geometry shown in Figure 1, where the two gaps $h_+(x)$ and $h_-(x)$ are small compared to the radius of the cylinder. The steady lubrication equations for the flow in the thin gaps are

$$\mu\frac{\partial^2 u}{\partial y^2} - \frac{\partial p}{\partial x} = 0, \qquad \frac{\partial p}{\partial y} = 0, \tag{2}$$

$$\frac{\partial u}{\partial x} + \frac{\partial v}{\partial y} = 0. \tag{3}$$

The solution of these equations for the given boundary conditions is standard. From equation (2), $p = p(x)$ only. Integrating twice and using the boundary conditions that on $y = 0$, $u = 0$, and on $y = h_+$, $u = \Omega a$, we find

$$u_+ = \frac{1}{2\mu}\frac{\partial p_+}{\partial x}\left(y^2 - h_+ y\right) + \frac{\Omega a y}{h_+}. \tag{4}$$

Note that y is measured from the wall to the cylinder, which in the top gap is downwards. The flow rate per unit width of channel is the same at every position x, and is found by integrating vertically across the gap using $q = \int_0^h u\, dy$, which for the top gap is

$$q_+ = -\frac{h_+^3}{12\mu}\frac{\partial p_+}{\partial x} + \frac{\Omega a h_+}{2}. \tag{5}$$

Since q_+ is constant, we solve for the total pressure drop by integrating $\partial p/\partial x$ along the gap from $-\infty$ to $+\infty$, finding

$$\Delta p_+ = -12 q_+ \mu \int_{-\infty}^{\infty} \frac{1}{h_+^3(x)}\, dx + 6\mu\Omega a \int_{-\infty}^{\infty} \frac{1}{h_+^2(x)}\, dx. \tag{6}$$

Making the approximation that locally the gap thickness varies quadratically as

$$h_+(x) = h_{o_+} + \frac{x^2}{2a} = h_{o_+}\left(1 + \frac{x^2}{2a h_{o_+}}\right). \tag{7}$$

where h_{o_+} is the minimum gap thickness, we find

$$\Delta p_+ = -\frac{9\sqrt{2}\pi\mu a^{1/2}}{2h_{o_+}^{5/2}} q_+ + \frac{3\sqrt{2}\pi\mu a^{3/2}}{h_{o_+}^{3/2}}\Omega. \tag{8}$$

Similarly, for the bottom gap,

$$\Delta p_- = -\frac{9\sqrt{2}\pi\mu a^{1/2}}{2h_{o_-}^{5/2}} q_- - \frac{3\sqrt{2}\pi\mu a^{3/2}}{h_{o_-}^{3/2}}\Omega. \tag{9}$$

Here we make the assumption that the total pressure drop across each gap must be equal since the cylinder is finite. The additional contributions to the pressure drop across the cylinder that derives from fluid motion outside the gap is expected to be $O(\mu q_{max}/a^2)$ where $q_{max} = \max(q_+, q_-)$, which is small compared to the corresponding terms in equations (8) and (9). Writing $\Delta p_+ = \Delta p_- = \Delta p$, we now have two equations with three unknowns: q_+, q_- and Ω. The torque is found by integrating the shear stress τ_{xy} over the surface of the cylinder, where $\tau_{xy} = \mu\partial u/\partial y\big|_{h_+}$, multiplied by the moment arm a,

$$L_+ = a\int_{-\infty}^{\infty} \tau_{xy}\big|_{h_+}\, dx = a\int_{-\infty}^{\infty}\left(\frac{1}{2}\frac{\partial p_+}{\partial x}h_+ + \frac{\mu\Omega a}{h_+}\right) dx. \tag{10}$$

Using equation (5) for $\partial p_+(x)/\partial x$ and the parabolic profile of the gap for $h_+(x)$, we integrate to find

$$L_+ = -\frac{4\sqrt{2}\pi\mu a^{3/2}}{h_{o_+}^{1/2}}\left(\frac{3}{4}\frac{q_+}{h_{o_+}} - \Omega a\right). \tag{11}$$

If the applied torque is L, and L_- is found as above, then for steady state operation $\sum L = 0$ yields

$$\frac{L}{4\sqrt{2}\mu} = \frac{a^{3/2}}{h_{o_+}^{1/2}}\left(\frac{3q_+}{4h_{o_+}} - \Omega a\right) - \frac{a^{3/2}}{h_{o_-}^{1/2}}\left(\frac{3q_-}{4h_{o_+}} + \Omega a\right). \tag{12}$$

It is convenient to non-dimensionalize all variables by using the average flow velocity q/a, the characteristic length a, and the shear viscosity μ. Also, it is useful to write $\delta = h_{o_+} + h_{o_-}$ and $\eta = h_{o_+}/\delta$, so $h_{o_+}/\delta = 1 - \eta$. The lubrication approximation requires $\delta \ll 1$. Notice that η varies from 0 to 1. Finally, the three equations for dimensionless q_+, q_- and Ω in terms of the geometrical factors η and δ are

$$-\frac{3q_+}{2\eta} + \Omega\delta = \frac{\Delta p \eta^{3/2}\delta^{5/2}}{3\sqrt{2}\pi}, \tag{13}$$

$$-\frac{3q_-}{2(1-\eta)} - \Omega\delta = \frac{\Delta p (1-\eta)^{3/2}\delta^{5/2}}{3\sqrt{2}\pi}, \tag{14}$$

and

$$\frac{3q_+}{\eta^{3/2}} - \frac{3q_-}{(1-\eta)^{3/2}} - \frac{4\left((1-\eta)^{1/2} + \eta^{1/2}\right)\Omega\delta}{\eta^{1/2}(1-\eta)^{1/2}} = \frac{L\delta^{3/2}}{\sqrt{2}\pi}. \tag{15}$$

The solution to these three equations yields

$$\Omega = \frac{\Delta p \delta^{3/2}}{3\sqrt{2}\pi}\left(\frac{(1-2\eta)\eta^{1/2}(1-\eta)^{1/2}}{\eta^{1/2} + (1-\eta)^{1/2}}\right) \tag{16}$$

$$-\frac{L\delta^{1/2}}{2\sqrt{2}\pi}\left(\frac{\eta^{1/2}(1-\eta)^{1/2}}{\eta^{1/2} + (1-\eta)^{1/2}}\right) \tag{17}$$

and summing q_+ and q_- to get the total flow rate q, which is unity because of our non-dimensionalization:

$$1 = -\frac{\sqrt{2}\Delta p \delta^{5/2}}{9\pi}\left(\eta^{1/2} + (1-\eta)^{1/2}\right)\left(3\eta^2 - 3\eta + 1\right) \tag{18}$$

$$+\frac{L\delta^{3/2}}{3\sqrt{2}\pi}\left(\frac{(1-2\eta)\eta^{1/2}(1-\eta)^{1/2}}{\eta^{1/2} + (1-\eta)^{1/2}}\right). \tag{19}$$

The four matrix elements in equation (1) can be found by taking the matrix of four coefficients for Δp and L above and inverting. One can see that the coefficients above are symmetric about $\eta = 1/2$, meaning that flows where the thinner gap is on the top are equivalent to

flows where the thinner gap is on the bottom, aside from some sign changes. The optimal geometry η_{max} for a given state can be found by finding the critical points of q, Ω, Δp, or L with respect to η, and will be reported in a paper being prepared.

A simple test to compare with the boundary integral results reported in the next section is the case where the rotation rate is zero, for which

$$\Delta p_\Omega = -\frac{9\pi}{\sqrt{2}\delta^{5/2}}\left(\frac{1}{\eta^{5/2}+(1-\eta)^{5/2}}\right) \tag{20}$$

and

$$L_\Omega = -\frac{3\sqrt{2}\pi}{\delta^{3/2}}\left(\frac{1-2\eta}{\eta^{5/2}+(1-\eta)^{5/2}}\right), \tag{21}$$

where the subscript denotes the zero-rotation case.

Solution using boundary integrals

The dimensionless boundary integral equation for Stokes flow (see [4]) in a volume of fluid V bounded by S is

$$\int_S \mathbf{n}\cdot\boldsymbol{\sigma}\cdot\mathbf{J}\,dS - \int_S \mathbf{n}\cdot\mathbf{K}\cdot\mathbf{u}\,dS = \begin{cases} \mathbf{u}(\mathbf{x_0}), & \mathbf{x_0}\in V \\ \frac{1}{2}\mathbf{u}(\mathbf{x_0}), & \mathbf{x_0}\in S \\ 0, & \mathbf{x_0}\notin V \end{cases} \tag{22}$$

where $\mathbf{n}$ is the unit normal pointing out of the fluid. For two-dimensional flows, the tensors $\mathbf{J}$ and $\mathbf{K}$ are

$$\mathbf{J} = \frac{1}{4\pi}\left(\mathbf{I}\log r - \frac{\mathbf{rr}}{r^2}\right),\ \mathbf{K} = \frac{1}{\pi}\frac{\mathbf{rrr}}{r^4}, \tag{23}$$

which are the fundamental solutions to Stokes flow due to a point force acting at $\mathbf{x_0}$, where $\mathbf{r} = \mathbf{x} - \mathbf{x_0}$ and $r = |\mathbf{r}|$. The boundary of the volume of fluid for this problem is shown in Figure 2.

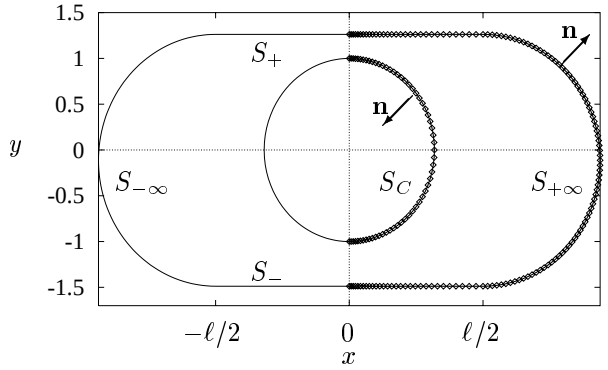

Figure 2: Boundary used for boundary integral solution: line is full contour of integration, and points show the half contour used in numerics when expoiting symmetry.

The boundary consists of two walls S_+ and S_- of length ℓ, two semi-circular arcs $S_{+\infty}$ and $S_{-\infty}$ at $x = \pm\ell/2$, and a circular cylinder S_C centered at the origin. Over $S_{+\infty}$ and $S_{-\infty}$, the fluid velocity is defined to be parabolic flow, denoted $\mathbf{U}_P$. Since the walls and the cylinder are rigid boundaries where $\mathbf{u}$ is defined, the integral involving $\mathbf{K}$ simplifies to

$$\int_{S_+ + S_-} \mathbf{n}\cdot\mathbf{K}\cdot\mathbf{u}\,dS = \int_{S_+ + S_-} \mathbf{n}\cdot\mathbf{K}\,dS\cdot\mathbf{U}_{\text{wall}} = 0, \tag{24}$$

and using $\mathbf{U_C} = \boldsymbol{\Omega}\wedge\mathbf{r}$,

$$\int_{S_C}\mathbf{n}\cdot\mathbf{K}\cdot\mathbf{u}\,dS = -\int_{S_C}\tilde{\mathbf{n}}\cdot\mathbf{K}\cdot\mathbf{U}_C\,dS = \int_{V_C}\delta(\mathbf{r})\boldsymbol{\Omega}\wedge\mathbf{r}\,dV, \tag{25}$$

where $\tilde{\mathbf{n}} = -\mathbf{n}$ is the normal pointing out of the cylinder, V_C is the volume of the cylinder, and $\nabla\cdot\mathbf{K} = -\mathbf{I}\delta(\mathbf{r})$ by definition of the fundamental solutions. So,

$$\int_{S_C}\mathbf{n}\cdot\mathbf{K}\cdot\mathbf{u}\,dS = \begin{cases} \mathbf{U}_C(\mathbf{x_0}), & \mathbf{x_0}\in V_C \\ \frac{1}{2}\mathbf{U}_C(\mathbf{x_0}), & \mathbf{x_0}\in S_C \\ 0. & \mathbf{x_0}\notin V_C. \end{cases} \tag{26}$$

As a result, the $\mathbf{K}$ integral over S_C only contributes $\frac{1}{2}\mathbf{U}_C$ when $\mathbf{x_0}\in S_C$ because V and V_C overlap only on S_C. The resulting boundary integral equations are

$$\int_S \mathbf{f}\cdot\mathbf{J}\,dS - \int_{S_{+\infty}+S_{-\infty}}\mathbf{n}\cdot\mathbf{K}\cdot\mathbf{u}\,dS = \begin{cases} \mathbf{U}_C(\mathbf{x_0}), & \mathbf{x_0}\in S_C \\ \frac{1}{2}\mathbf{U}_P(\mathbf{x_0}), & \mathbf{x_0}\in S_{\pm\infty} \\ 0, & \mathbf{x_0}\in S_\pm \end{cases} \tag{27}$$

where $\mathbf{n}\cdot\boldsymbol{\sigma}$ has been written as $\mathbf{f}$ to represent the unknown traction acting on the boundary.

To solve equations (27) for $\mathbf{f}$, the boundary is discretized into n nodes, as shown on the right side of Figure 2, which are described using an arclength-like parameter s that increases clockwise along the outer and inner boundaries. The unknown force $\mathbf{f}$ is approximated linearly by

$$\mathbf{f}(s) = \sum_{k=1}^{n} w_k(s) f_{xk}\hat{\mathbf{e}}_x + \sum_{k=1}^{n} w_k(s) f_{yk}\hat{\mathbf{e}}_y \tag{28}$$

where the weight function w_k for is defined by

$$w_k(s) = \begin{cases} 1-|s-k| & k-1\le s\le k+1 \\ 0 & (s<k-1)\cup(k+1<s). \end{cases} \tag{29}$$

The boundary is described simply using lines and circular arcs, with a nodal spacing that varies quadratically along S_C and $S_\pm$. A set of $2n$ linear equations is generated by taking $\mathbf{x_0}$ to be each node $\mathbf{x}_k$ and solving both components of equation (27) for the unknowns f_{xk} and f_{yk} at each node. The left-right symmetry of the problem is exploited to reduce the computation time by a factor of 8. The code was checked using Poiseuille flow, corresponding to the case where the radius of the cylinder is zero, and Couette flow [5] corresponding to the case where $q = 0$ and the length of the wall $\ell = 0$.

The two input variables are the flow rate q and the rotation rate of the cylinder Ω. Taking $q = 1$ and $\Omega = 0$, the unknown f_{xk}'s and f_{yk}'s are calculated. The resulting pressure drop across the cylinder Δp is

$$\Delta p = f_y(\ell/2) - f_y(-\ell/2) - \frac{12\ell}{(2+\delta)^3} \tag{30}$$

which is independent of ℓ and where the last term is the pressure drop one would have in the channel only due to Poiseuille flow in a channel of height $2+\delta$. Figure 3 shows a typical plot of f_y, which at the planar wall is equal to the pressure.

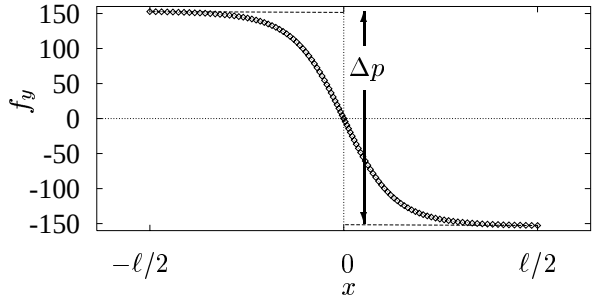

Figure 3: Vertical component of $\mathbf{n}\cdot\boldsymbol{\sigma} = f_y\mathbf{e_y}$, equal to the pressure in the fluid at the wall. The pressure drop is defined as the difference in pressure at $x = \pm\ell/2$ minus the pressure drop due to Poiseuille flow over a length ℓ. This simulation had net torque equal to zero.

The resulting torque is found by integrating the tangential stresses over the surface of the cylinder,

$$L = \int_0^{2\pi} (f_y \cos\theta - f_x \sin\theta)\, d\theta. \tag{31}$$

The torque for the case $\Omega = 0$ is denoted L_Ω, and the pressure drop Δp_Ω. Figures 4 and 5 show that the numerical solution indeed approaches the lubrication limit as δ becomes small.

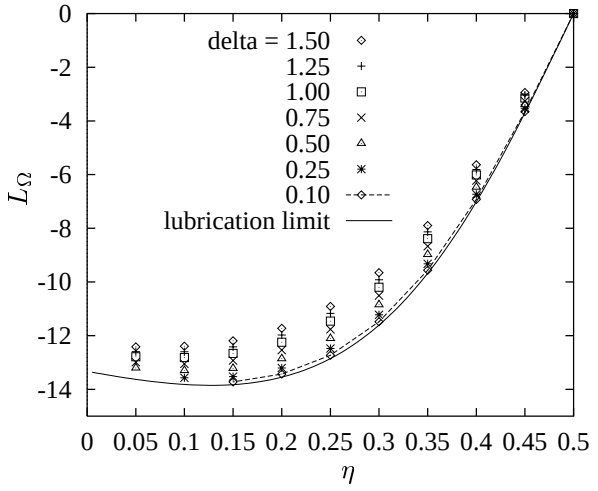

Figure 4: Torque from boundary integral simulations where the rotation rate is zero, for various δ at several η. As δ becomes small, L_Ω approaches the lubrication limit.

To find Ω_L, the rotation rate where $L = 0$, we use the fact that torque is a linear function of Ω. Solving for a second point (Ω, L), we can extrapolate linearly to find Ω_L, and solve the system a third time. The

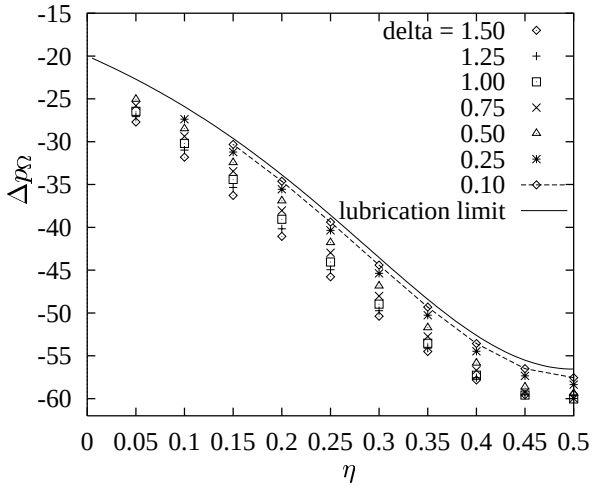

Figure 5: Pressure drop from boundary integral simulations where the rotation rate is zero, for various δ at several η. As δ becomes small, Δp_Ω approaches the lubrication limit.

pressure drop, maximum wall shear stress and Ω_L can all be compared to the lubrication limit for zero net torque. Details of the agreement between lubrication theory and the BIM for the cases of zero torque and non-zero rotation are described in a paper being prepared.

Conclusions

We have used the lubrication approximation to show that the general solution for the flow over a rotating cylinder in a two-dimensional channel can be found in terms of four parameters: q, Ω, Δp, and L. Boundary integral methods are demonstrated to be suitable for this problem where resolution in the thin gaps is important. The BIM solution found numerically is shown to approach the lubrication limit for the case of zero rotation, and the relative difference is approximately 2% for $\delta = 0.1$, where the sum of the gaps is 10% of the radius of the cylinder. For the purposes of designing MEMS, the optimal geometry η_{max} can be found for a given state and is to be reported in a paper in preparation.

REFERENCES

[1] M. Sen, D. Wajerski, and M. Gad-El-Hak, Trans. ASME J. Fluids Eng. **118**, 624 (1996).

[2] M. C. Sharatchandra, M. Sen, and M. Gad-El-Hak, Trans. ASME J. Fluids Eng. **119**, 372 (1997).

[3] D. DeCourtye, M. Sen, and M. Gad-El-Hak, Int. J. Comp. Fluid Dyn. **10**, 13 (1998).

[4] J. Tanzosh, M. Manga, and H. A. Stone, in *Proceedings of Boundary Element Technologies VIII*, edited by C. A. Brebbia and M. S. Ingber (Computational Mechanics Publications, UK, 1992), pp. 19–39.

[5] G. K. Batchelor, *An Introduction to Fluid Dynamics* (Cambridge University Press, UK, 1967).